International Journal of Ecology and Environmental Sciences 51: 449-470, 2025
ISSN: 2320-5199 (Online); https://doi.org/10.55863/ijees.2025.0707

Assessment of Thermal Comfort and Heat Risk in Predominant Urban Heat Islands of Paschim Bardhaman District, West Bengal, India

MOUMITA HATI, Y.V. KRISHNAIAH*, DEBASIS DAS, MANIKA MALLICK, VAJANA MONDAL, KAUSIK PANJA AND ATOSHI CHAKMA

Department of Geography and Disaster Management, Tripura University (A Central University), Suryamaninagar, 799022, Tripura, India

Email: moumitahati421997@gmail.com; yvkrishna09@gmail.com; yvkrishnaiah@tripurauniv.ac.in; debasisdas379@gmail.com; mnkmlik14@gmail.com; bhajana.1995@gmail.com; kausikpanja89@gmail.com; atoc.chakma@gmail.com

ORCID ID: 0009-0000-8699-0890 (MH), 0000-0002-8335-6533 (YVK), 0009-0000-0175-1445 (DD), 0000-0003-2768-2673 (MM), 0009-0009-9283-2384 (VM), 0009-0007-5098-2056 (KP), 0009-0008-7438-3370 (AC)

***Corresponding author**

ABSTRACT

The current study assesses the influence of land use changes in one of India's most important metropolitan zones to understand better the relationship between land use practices and urbanization and the rising trend of land surface temperature. Quantify the geographical changes in land use land cover (LULC) and Urban Heat Island (UHI) of the Paschim Bardhaman for 30 years (1991-2021) using multi-temporal satellite and field data. RS data from 1991, 2001, 2011, and 2021 were used to derive land cover maps, analyze LST, develop danger maps, and use GIS to connect land cover change to LST. Between 1991 and 2021 the built-up area of Asansol increased by 29.5% replacing agricultural land and vegetation area. LST found in the study area is much more prominent in the core part of city than in the surrounding areas. Urban heat islands grew by 9.42% between 1991 and 2021. Between 1991 and 2021, 'excellent' ecological regions decreased by 4.49%, while 'bad,' 'worse,' and 'worst' areas increased by 10.84%, 'good' and 'normal' areas decreased by 6.61%. The outside parts of Asansol City, Raniganj, Andal, and Durgapur are more susceptible, accounting for 14.92% of the district. The core region of Asansol and Kulti, which has a large population density, faced high heat danger due to overcrowding, inadequate air circulation, and excessive traffic.

Key words: Ecological evaluation index, Heat risk index, Land surface temperature, Urban thermal field variance index, Urban heat island, Paschim Bardhaman

INTRODUCTION

Land Surface Temperature (LST) is a crucial parameter because of its capacity to affect biological, chemical, and physical processes on Earth; it is also required for studies on urban climate (Pu et al. 2006). LST is extremely sensitive to varying land coverings. Increased urbanization contributes significantly to land cover changes and substantially impacts the region's LST, which might disrupt the ambient habitat of our ecosystem (Zhou et al. 2022). UHI's geographical and temporal changes are influenced by impervious surface area, landscape structure, plant cover, albedo, and climate. Several researchers have attempted to ascertain the relationship between LST and other land cover factors or indices (Imram et al. 2021). Given that the plant cover significantly affects urban LST, it is crucial to examine the relationship between LST and vegetation indices (Amiri et al. 2009, Mathew et al. 2016). Understanding LST and how it varies in space and time is crucial for comprehending how human activity and the environment interact. LST fluctuates quickly in both space and time. LST varies fast in space and time, and understanding LST and its spatial and temporal variations is critical for understanding the connections between human activities and the environment (Haldar et al. 2022). The night LST maps indicate clear UHI patterns in semiarid regions that were not visible on the day LST maps, and UHI is caused by urbanization (Zhou et al. 2015, Yang et al. 2015). As a result, night LST maps will be more relevant for investigating the impact of urbanization on UHI in semiarid regions. During the summer or

before the monsoon season, most Indian towns act like desert or semiarid environments (Shastri et al. 2019). Night LST maps are more appropriate for UHI investigations in various Indian cities.

The urban heat island effect is when the surface temperature in urban areas is higher than in surrounding non-urban areas (Oke 1973). Urban Heat Island (UHI) refers to the warm characteristics of a town or city. Anthropogenic activity influenced the surface and atmospheric elements associated with urban development, leading to unintended climatic change. Air temperature is related to UHI, but its occurrence and temporal variation may differ (Oke 1995, Mathew et al. 2016). Urbanization in India has been at a rapid pace since post-independence, as proved by the estimates that the population living in cities in 1901 was 11.4% and has increased by 30% as per the 2011 census in India. The built-up area increased nearly 2.5 times from 1991 to 2018 (Bhatta 2009). The most popular method for identifying the effects of urbanization on temperature is to compare the temperature differences between urban and rural sites (Yague et al. 1991, Jauregui et al. 1992, Karaca et al. 1995, Sultana and Satyanarayana 2019). Rapid urbanization (Chakma et al. 2023, Mallick and Krishnaiah 2023) leads to the UHI phenomena all over India, especially in metropolitan cities (Shahfahad et al. 2022). Heat-related mortality was higher in urban centers than in the periphery (Tan et al. 2010). Also, people's physiological health and productivity are affected, especially outdoor workers, due to extreme temperatures (Barata 2011, Fouillet 2008).

The Urban Thermal Field Variance Index (UTFVI) concentration is higher where the area is substantially warmer than the surrounding rural areas (Wang et al. 2016). The UTFVI is a widely used indicator for evaluating the eco-environmental quality of urban areas and thermal well-being. Declining air quality, spatial and temporal variations in humidity, decreasing thermal comfort, increasing death rates, changing local wind patterns, thunderstorm activity, and shifting rainfall patterns are the leading causes of decreased ecological comport value of the area (Degerli and Cetin 2023). The highest influence of UTFVI value was observed in mines and urban areas, while vegetation cover had the least impact. The UHI can be a valuable tool for identifying the consequences of UTFVI on the city by identifying hotspots and assisting urban planners in developing measures.

Land surface temperature varies from city to city, depending on unique characteristics. Asansol Durgapur Development Region's land surface temperature mostly varied from 32 to 58°C in summer due to planned and unplanned city growth and new mines and industries (Gupta et al. 2019, Mohan et al. 2020). Asansol Municipal Corporation experienced rapid population growth in the surrounding area, with unplanned and haphazard growth of cities (Maity et al. 2020). In Paschim Bardhaman, random mining pits are opening in many areas (Anonymous 2015), significantly decreasing forest cover and increasing the built-up area and barren land, which prolonged the urban heat island formation (Chatterjee and Gupta 2021). From 1993 to 2018, in the Asansol subdivision area, coal mines and urban areas significantly increased by 15 and 60%, respectively (Das et al. 2021). Mining activities also adversely affected the agriculture of surrounding areas (Hota and Behera 2015). The green space in cities is decreasing gradually, which can create a long-term impact on ecology and the water budget (Siddique et al. 2020). The severity of heat waves demands irrigation for agriculture since it negatively impacts crop production (Kumar et al. 2017, Siebert et al. 2017). Agriculture and irrigation practices largely control the magnitude of urban-rural temperature contrasts (Gupta et al. 2024).

MATERIAL AND METHODS

Study area

In Paschim Bardhaman district is predominantly mining, industrial and the most urbanized areas are Asansol, Salanpur-Kulti, Chrulia, Andal-Raniganj and Durgapur have experienced higher LST compared to rural surrounding areas. Previously, this area was under a dense forest named 'Jangal Mahal' (Paterson 1910), and in Raniganj East India, the company started its first coal mine in 1774 (Koshal 2002). After that, significant changes in natural elements are recorded. After 2001, approximately 70% of opencast mines were initiated (Patra et al. 2022). The first industry was established in 1871, the Indian iron and steel company in Kulti, which is

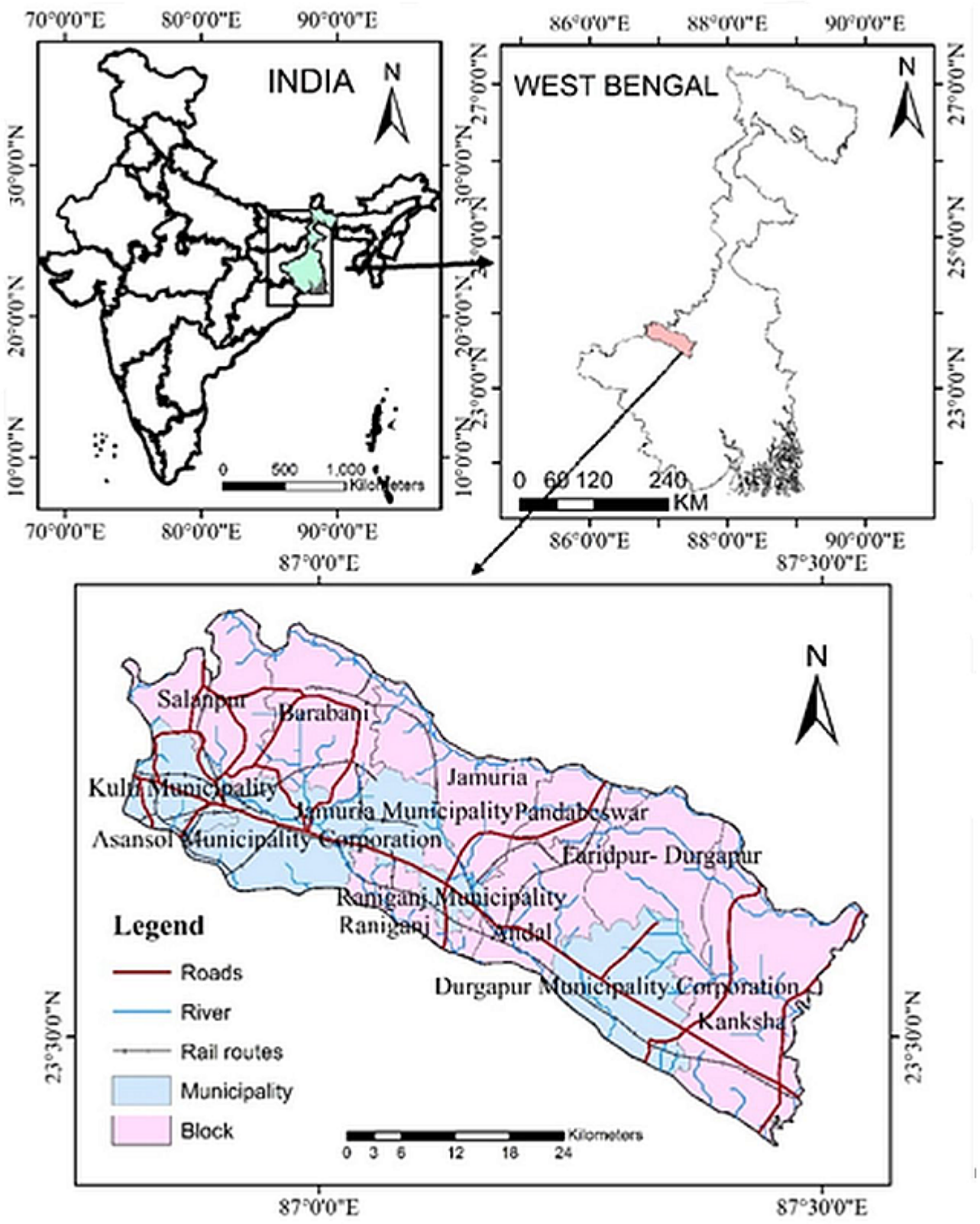

Figure 1. Location map of the study area

situated in the Asansol subdivision. Previously, it was adjoined with the Bardhaman district. After 2016, it was separated and formed as the 23rd district of West Bengal. The district lies between 23°25' to 23°40'N and 86°40' to 87° 30'E, which comprises an area of 1603.17 km^2 (Fig.1). Paschim Bardhaman is situated in the western part of West Bengal and is popularly known as 'Rarh Banga'. The district shares borders

with Birbhum in the north, Bankura and Purulia in the south, Purba Bardhaman in the east, and Jharkhand state in the west. Paschim Bardhaman district is naturally bounded by the Ajay and Damodar Rivers in the north and south. Barakar River and Maithan Dam are located in the western part of this area. The mean temperature of Paschim Bardhaman district is 32.5°C. The daytime temperature reached its maximum in May (37.4°C), but night temperature was recorded as high from June to September (25.6°C). Chota Nagpur Plateau dominates the study area in the west, and an eastern boundary comprises young and older alluvium. The study area is in a transition zone between the western plateau and the eastern alluvial plain.

Data sources and analysis methods

Spectral reflectance images from the United States Geological Survey (https://earthexplorer.usgs.gov/) were obtained online. Atmospherically and geometrically corrected bands for the Thematic Mapper (Landsat-5), Enhanced Thematic Mapper + (ETM), and Operational Land Imager (Landsat-8) are retrieved for the years 1991, 2001, 2011, and 2021.

Land surface temperature (LST)

$$LST = BT/(1+\lambda * (BT/P) * \ln(E))$$

To extract LST, parameters viz., Top of Atmosphere (ToA), Brightness of Temperature (BT), NDVI, Land Surface Emissivity (LSE), and Proportion of Vegetation (PV) were used.

i) ToA: The Landsat 4-5 (TM) for the years 1991, 2001, and 2011, and Landsat 8 OLI/TIRS for the year 2021 sensor is manually converted into Top of Atmosphere (ToA) radiance by applying the equations for LANDSAT 4-5 and for LANDSAT 8 OLI/TIRS

$$L\lambda = ((LMAX\lambda - LMIN\lambda)/(QCALMAX - QCALMIN))*(QCAL-QCALMIN) + LMIN\lambda) \quad \text{...(Landsat 4-5)}$$

$$L\lambda = ML*QCAL+AL \quad \text{.....(Landsat 8)}$$

ii)BT

$$BT = K2/(\ln(K1/L\lambda)+1))-273.15$$

iii) NDVI

$$NDVI = (NIR-RED)/(NIR+RED)$$

iv) Land surface emissivity (LSE)

$$P\upsilon = ((NDVI-NDVImin)/(NDVImax-NDVImin))^2$$

Where, Pυ= Proportion of vegetation, NDVI= DN value from NDVI image, NDVImin = Minimum DN value of NDVI image, NDVImax = Maximum DN value of NDVI image.

$$E = 0.004 * P\upsilon + 0.986$$

Where E= Land Surface Emissivity, Pυ= Proportion of vegetation, 0.004 and 0.986 correspond to correction values of the equation.

UHI and Non-UHI

The following equations were used to determine Urban heat island (UHI) and Non-UHI zonation (Guha et al. 2018, Fahmy et al. 2023)

$$Non\ UHI = 0 < LST < \mu + 0.5 * std$$

$$UHI = LST > \mu + 0.5 * std$$

where μ is the mean LST denote and std is the Standard Deviation (SD) of LST in Paschim Bardhaman, respectively. Using the above UHI, zones were derived as the areas with LST higher than the sum of the mean LST and $\mu + 0.5 * std$. These are the warmest parts of the region. The remainder of the governorate is non-UHI, according to the equation. Based on UHI and Non UHI threshold LST five most dense UHI Zones were identified i.e., Asansol Urban area, Salanpur- Kulti, Churulia mines area, Andal-Raniganj area, and Durgapur.

Landuse and land cover

Spatio-temporal variation of LULC was detected for the years 1991, 2001, 2011, and 2021 using LANDSAT 4-5 and 8-9 satellite images with the help of Supervised and Unsupervised classification using Maximum likelihood Algorithm and k-means method using the software QGIS 3.6.18. 1991-2021 (Mallick et al. 2024, Panja et al. 2023)

Urban thermal field variance index (UTFVI)

For the Paschim Bardhaman, the Urban Thermal Field Variance Index (UTFVI) was computed to define the impact of UHI quantitatively. UTFVI was calculated using the following formulas derived from (Yong et al. 2006, Rashid et al. 2022).

$$UTFVI = (T\ LST - T\ mean)/(T\ mean)$$

Where T LST = Land Surface Temperature, T mean = Mean temperature of the area

Heat risk index

The following equation assesses the study area's heat

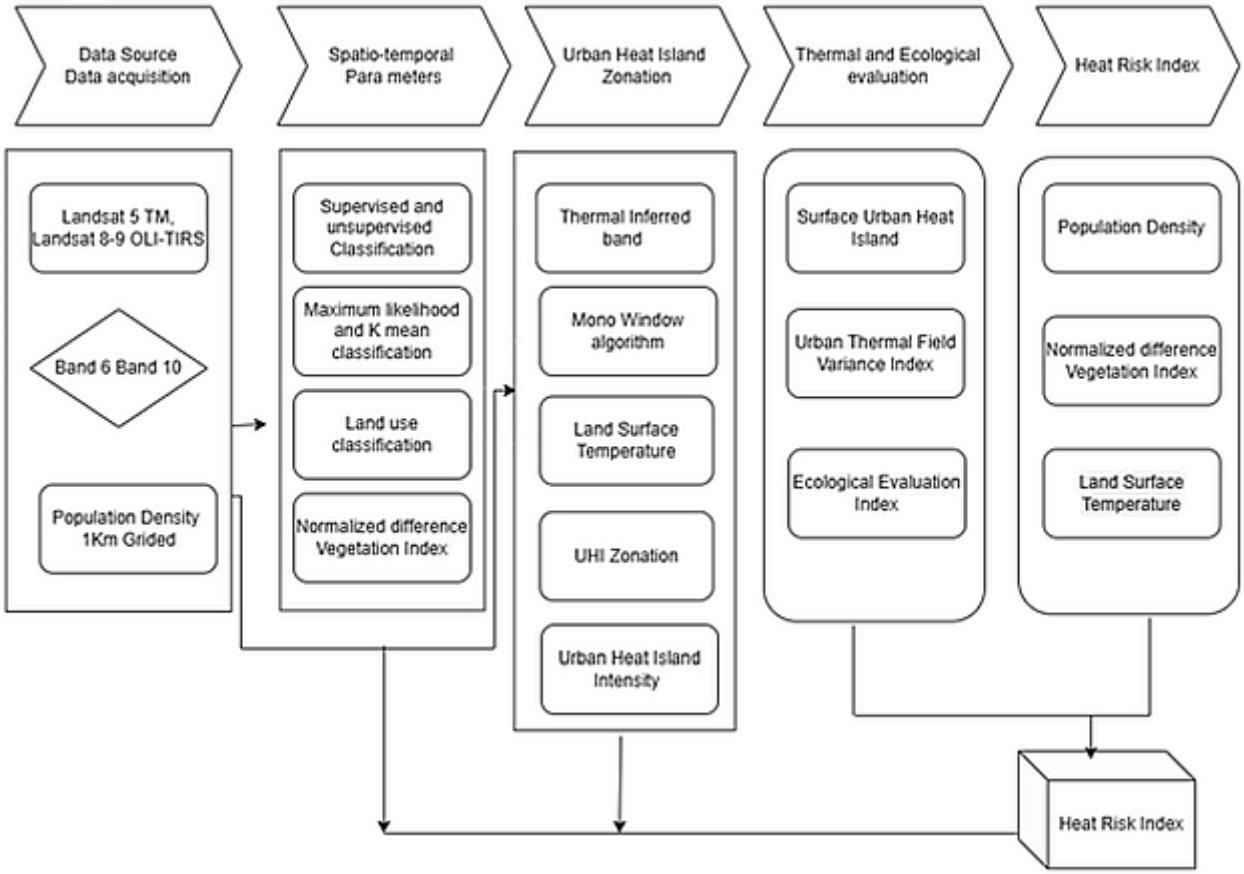

Figure 2. Methodological framework

risk Index (Aubrecht and Özceylan 2013, Yardley et al. 2011).

Population density + Vegetation cover + Land surface temperature

The population density was determined by the 1 km gridded population data of 2021. The Normalised Difference Vegetation Index was used for vegetation cover, and the mean land surface temperature of 2021 was used to calculate the temperature.

RESULTS AND DISCUSSION

Mean land surface temperature (1991to 2021)

In 1991, 2.11% of the study area experienced less than 25°C, and 41.33% of the area between 25-27°C, mainly the south-eastern part of the study area, which is less populated and densely vegetated. Maximum area of the district (47.22%) experienced 27-29°C LST. Only 8.69% area experienced up to 31°C during this period. However, in 2001, areas under 25 and 27°C declined by 0.56% and 22.07%, respectively, while areas under 27-29, 29-31, and 31-33°C increased by 8.16, 12.57, and 1.87%, respectively. In 2011, more than 60% of the study area experienced more than 29°C LST. Over time, the area under high temperature increased rapidly in the core city region and the mining area. In 2021, only 0.58% of the area experienced less than 27°C, while the area under 29-31°C decreased from 60.70 to 36.53%. However, 54.10% of the area experienced 31-33°C LST. In 1991, no area was in the 33-35°C range, but in 2001, 0.03% of the area fell under this range, which is very minimal. However, in 2021, 4.36% of the area experienced higher than 33°C LST. Similarly, more than 35°C LST was observed in 0.46% area (Table 1, Fig. 3).

Temporal variation of UHI and non UHI area in Paschim Bardhaman district (1991 to 2021)

The rise in temperature through anthropogenic activity in any area is called the Urban Heat Island (UHI) effect (Gazi and Mondal 2018). This UHI

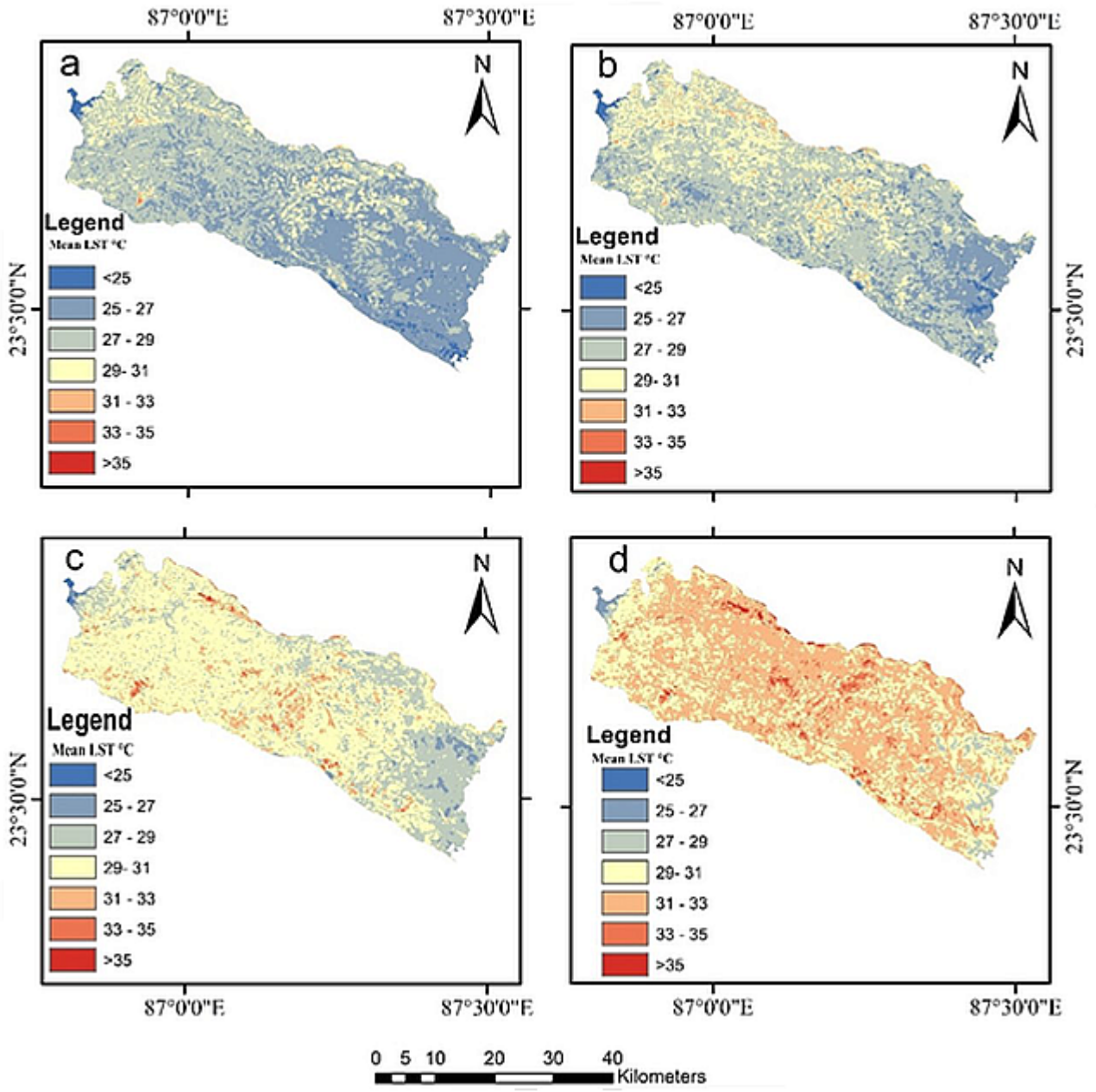

Figure 3. Spatio temporal variation of mean LST of the Paschim Bardhaman District (a.1991 b. 2001, c.2011 d.2021)

Table 1. Spatio-temporal variation of area of LST in Paschim Bardhaman District (1991-2021)

LST	1991		2001		2011		2021	
(°C)	Area (km^2)	Area (%)	Area (km^2)	Area (%)	Area (km^2)	Area (%)	Area (km^2)	Area (%)
<25	34.16	2.11	25.07	1.55	3.13	0.19	0	0
25-27	666.15	41.33	310.43	19.26	31.71	1.96	9.49	0.58
27-29	761.01	47.22	892.3	55.38	443.89	27.55	63.57	3.94
29-31	140.14	8.69	342.67	21.26	978.07	60.70	588.57	36.53
31-33	10.11	0.62	40.14	2.49	139.64	8.66	871.7	54.10
33-35	0	0	0.49	0.030	13.67	0.84	70.25	4.36
>35	0	0	0.04	0.0024	1.03	0.063	7.53	0.46

effect is mainly created by the concentration of human activities and artificial built surfaces, which are primarily, composed of impervious construction materials that absorb and store solar energy, slowly releasing heat, mainly during the night. The urban heat island effect is crucial for air quality control and environmental degradation (Guha et al. 2018, Fahmy et al. 2023). The severity of an urban heat island is determined by the temperature differential between its surrounding area and the center region. According to the findings, the geographical distribution of UHI exhibited a very constant pattern throughout the study (Kikon et al. 2016). A more significant effect of UHI was seen in Asansol, Durgapur urban industrial area, Andal, Jamuria urban industrial mining area, Salanpur mining area, and Churulia mining area during these periods.

The temporal structure of UHI areas has changed during the decade-wise study; their severity has increased in the center due to the expansion of built-up areas and the decline in vegetation. Urban areas, barren terrain, industrial areas, and, most importantly - mining areas are also contributing to the increase of UHI. In Paschim Bardhaman, the UHI threshold temperature rose between 1991 and 2021 by +3.84°C. The mean LST values increased significantly between 1991 and 2021. From 1991 to 2021, there was a more significant rise of 4°C in the maximum LST values in UHI locations. The mean and lowest LST values rise less than the maximum LST values, which climbed in non-UHI zones. In 1991, LST was greater than UHI in 14.48% of the area. It has a surface area of around 232.18 km^2, steadily expanding. In 2001, the UHI area was 18.19%, while the non-UHI area decreased by 3.71% from 1991. This trend continued in 2011 and 2021, but in 2021 UHI area abnormally increased from 14.48 to 23.90% (+9.42%). The UHI area grew at an annual rate of 0.15% (Table 2, Fig. 4).

LULC association with LST of predominant UHI areas

A detailed study of the formation of UHI in five predominant areas in the Paschim Bardhaman district was conducted. These areas are selected based on the effectiveness of temperature, built-up, industries, mining, and open barren land. The names of the five areas are Asansol, Salanpur-kulti, Churulia Mining, Andal-Raniganj, and Durgapur urban industrial areas.

Asansol Urban Heat Island and land use land cover (1991-2021)

The A-B cross-section of the Asansol area shows growth in urban heat island phenomena from 1991 to 2021. It has demonstrated clearly that the central area of Asansol City shows the most significant temperature rise over time due to the pressure of urban population agglomeration and industrial hub (Krishnaiah 2013, Mallick et al. 2025). Further, the emissions of large quantities of heat and water vapour from the Indian Iron and Steel Company (IISCO) and other heavy iron and steel factories cause the LST to increase to 36°C. The LST gradient reduces from core to peripheral areas.

Vegetation decreased drastically from 27.83% in 1991 to 6.70% in 2021 and decreased gradually from 12.20% in 2001 to 11.01% in 2011. The Asansol region's build-up area increased from 22.35% in 1991 to 32.42% in 2001, 44.77% in 2011, and 51.85% in 2021. Mainly, vegetation cover decreased, and built-up area increased through the National Highway-2 and Asansol-Burnpur road from the core to the peripheral region. Agricultural land increased from 43.48 to 55.82% between 1991 and 2001. However, in 2011 and 2021, it decreased by 36.48

Table 2. Temporal variation of UHI and non UHI area in Paschim Bardhaman District (1991 to 2021)

Years	Mean temperature (°C)	Threshold temperature (°C)	UHI area (km^2)	Non UHI area (km^2)	UHI area (%)	Non UHI area (%)
1991	27.30	27.94	232.18	1378.22	14.48	85.52
2001	28.08	30.02	291.65	1318.75	18.19	81.81
2011	29.60	30.39	340.92	1269.48	21.26	78.74
2021	31.14	31.75	382.28	1227.12	23.90	76.10

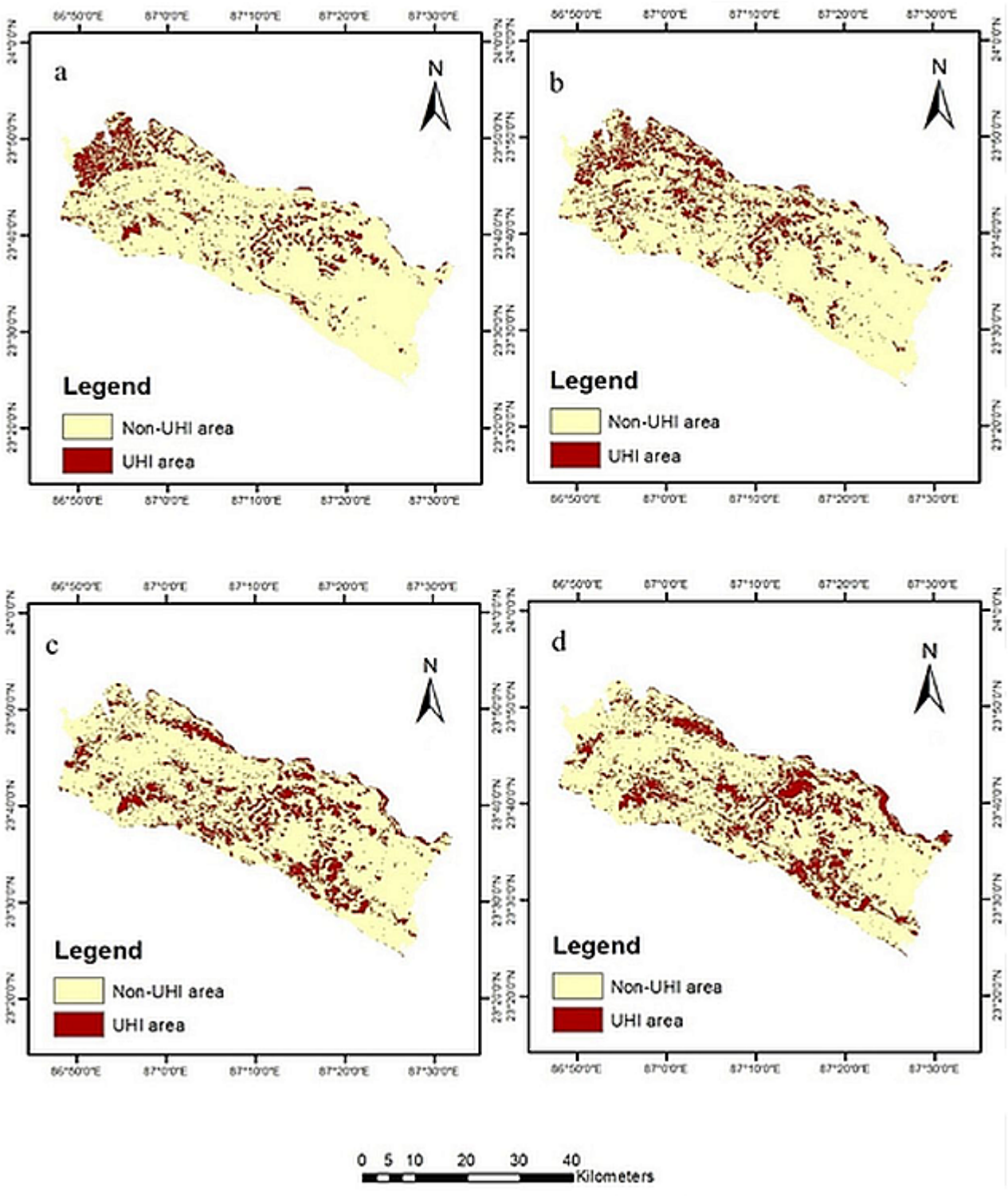

Figure 4. Spatio-temporal variation of UHI and non UHI area in Paschim Bardhaman District (a. 1991, b. 2001, c. 2011, d. 2021)

and 30.61%, respectively, in the south and south-western parts along the Asansol-Burnpur road. The Asansol region has many heavy industries, especially iron and steel. IISCO steel plant is located in the southwest part of the study area. Industrial area increased by 9.91% in 1991, 3.94% in 2001, 5.23% in 2011, and 6.45% in 2021. Very negligible opencast mining activity was found in the Asansol region. Water bodies and barren land experienced increasing and decreasing trends due to changes in water volume

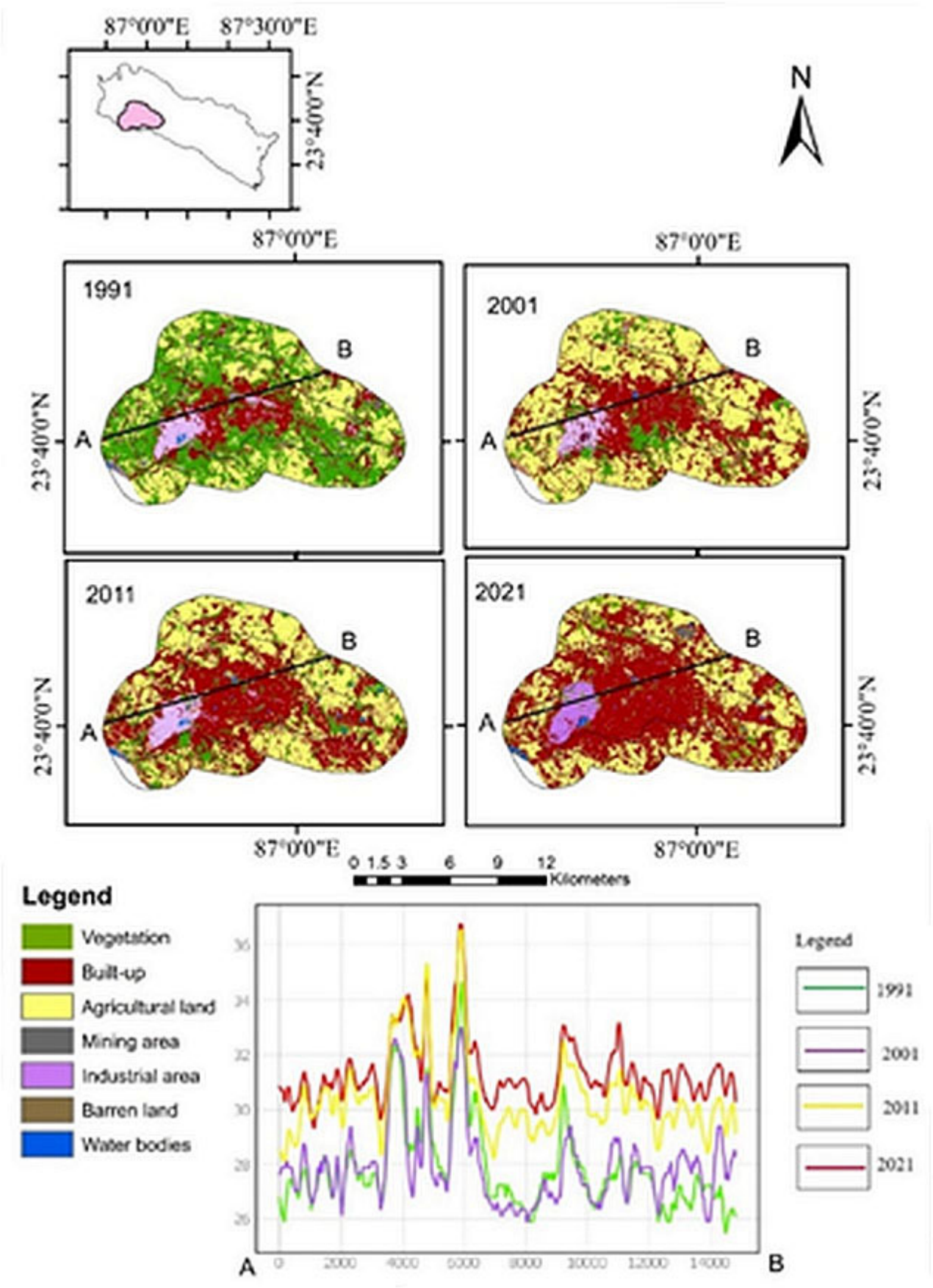

Figure 5. UHI map of Asansol region (1991 to 2021)

Table 3. Land use and land cover changes of Asansol area (1991- 2021)

LULC classes	1991		2001		2011		2021	
	Area (km^2)	Area (%)	Area (km^2)	Area (%)	Area (km^2)	Area (%)	Area (km^2)	Area (%)
Vegetation	42.68	27.83	18.68	12.20	16.85	11.01	10.3	6.70
Built-up area	34.28	22.35	49.62	32.42	68.5	44.77	79.66	51.85
Agricultural land	66.68	43.48	72.74	47.52	55.82	36.48	47.03	30.61
Mining area	0.5	0.32	0.65	0.42	1.05	0.68	1.44	0.93
Industrial area	6.01	3.91	6.04	3.94	8.01	5.23	9.91	6.45
Water bodies	1.08	0.70	2.05	1.33	0.92	0.60	4.38	2.85
Barren land	2.1	1.36	3.27	2.13	3.84	2.50	0.91	0.59

and sand deposition in the Damodar River (Table 3, Fig. 5).

Salanpur and Kulti UH and LULC (1991-2021)

Some parts of the Kulti municipality area and the Salanpur CD block are in this region. In the western part, most areas have been modified due to urbanization and the expansion of industrial areas. This region was previously covered with vegetation and settlements in 1991; however, after the establishment of coal mines, the land use drastically changed. The C-D cross-section area of this area experienced rising temperature trends from 1991 to 2021. Maximum temperature reached above 34°C in 2021 (Fig. 6). LST began to rise as the built-up area and mining region expanded in this cross-section. Dense vegetation cover decreased in the western and southwestern parts (Salanpur-Kulti area), 25.78% in 1991, 16.46% in 2001, 9.54% in 2011, and 9.47% in 2021. Built-up area increased rapidly from 13.02% in 1991, 15.13% in 2001, 23.10% in 2011, and 36.94% in 2021, respectively, on the bank of Barakar River. Agricultural land increased from 49.85% in 1991 to 55.51% in 2001 and decreased 8.1% between 2011 and 2021. The change is apparent in the central part of this region, predominantly due to mining activity done by Eastern Coalfield Limited (ECL) and Bharat Coking Coal Limited (BCCL). The mining area increased from 4.75% in 1991 to 6.59% in 2011. Active coal mine area decreased in 2021, and some land was occupied for settlements (Table 4, Fig. 6).

Churulia mines UHI and LULC (1991-2021)

This region is located to the north of the study area. It was once a densely forested region, but after 2001, new opencast coal mines were established here. The E-F cross-section area from 1991 clearly shows no strong temperature gradient, and peak LST ranged from 25 to 34°C (Fig. 7). However, temperature is expected to increase by 2021 due to coal mines in the area. This location was surrounded by agricultural land, vegetation, and River Ajay, with minimal built-up area. The vegetation cover of the Churulia region decreased gradually from 1991 to 2021. In 1991, 13.19% area was covered with dense vegetation, but in the next three decades, it decreased to 9.20% in 2001, 8.59% in 2011, and 8.12% in 2021 in the northern part. Built-up area increased from 3.23% in 1991 to 3.69% in 2001, 6.59% in 2011, and 15.86% in 2021. The built-up area's maximum growth (9.27%) occurred between 2011 and 2021. Agricultural land decreased gradually from 68.01% in 1991 to 61.68% in 2021. After the mining area's opening on the Ajay River bank, it rapidly expanded from 1.78% in 1991 to 9.48% in 2021. The mining area further expanded into surrounding agricultural land. Riverside barren land and current agricultural fallow land also rapidly decreased to 17.39% in 2001, 11.17% in 2011, and 3.75% in 2021 and converted into coal mines (Table 5, Fig. 7).

Raniganj and Andal UHI and LULC (1991-2021)

The Raniganj-Andal region is situated in the central parts of the study area. Dense built-up, mining, and industrial areas in the west primarily define this area. Maximum increase in LST was seen in the center, the mining, and industrial regions. The intensity of the UHI was relatively low in 1991, and the temperature gradient was also not substantial in the cross-section G-H. However, by 2021, this area experienced an urban heat island phenomenon

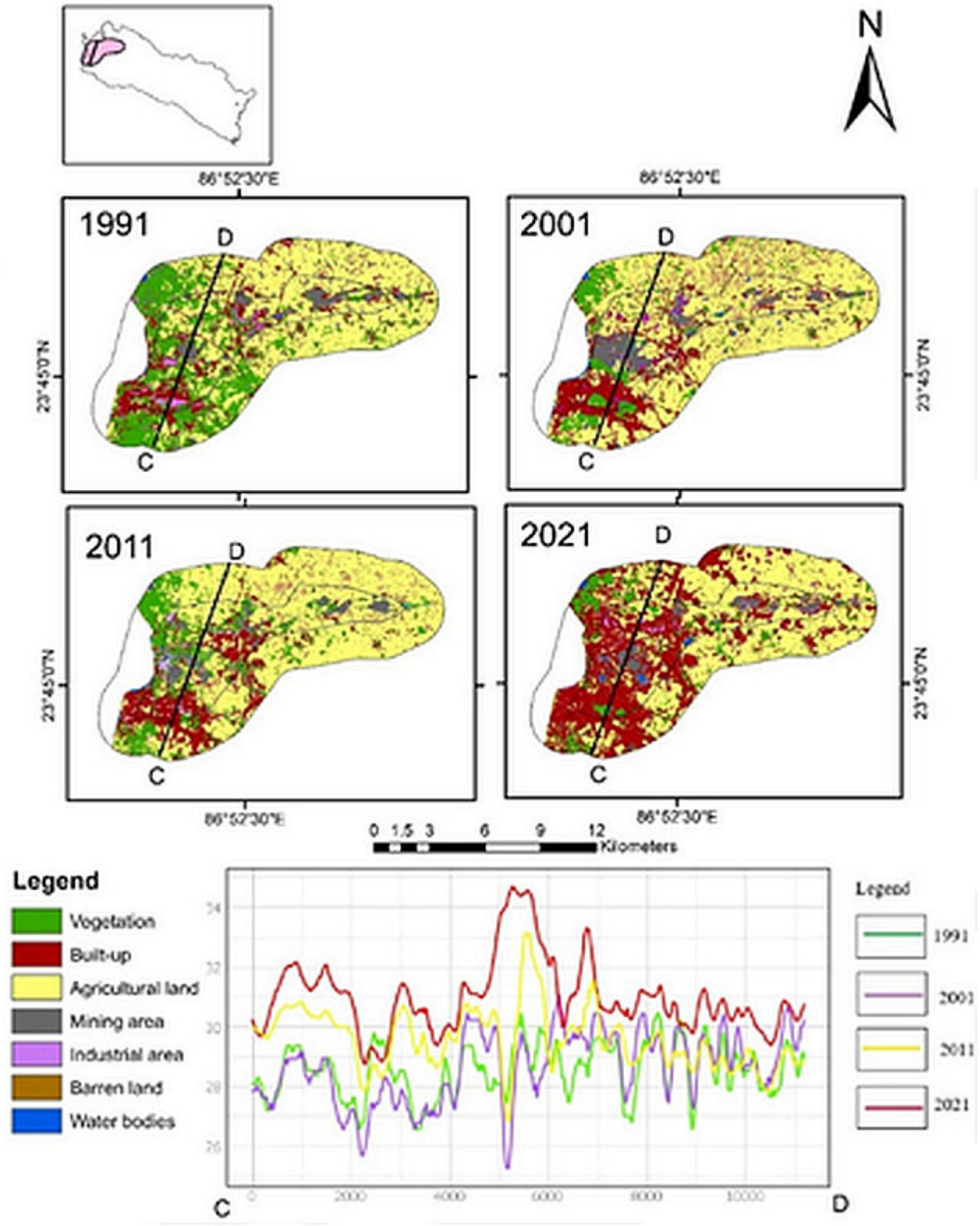

Figure 6. UHI map of Salanpur-Kulti region (1991 to 2021)

Table 4. Land use and land cover change of Salanpur-Kulti area (1991- 2021)

LULC classes	1991		2001		2011		2021	
	Area (km^2)	Area (%)	Area (km^2)	Area (%)	Area (km^2)	Area (%)	Area (km^2)	Area (%)
Vegetation	30.80	25.78	19.63	16.46	11.32	9.54	11.24	9.47
Built-up area	15.56	13.02	18.04	15.13	27.41	23.10	43.84	36.94
Agricultural land	59.56	49.85	66.19	55.51	63.35	53.39	53.75	45.29
Mining area	5.68	4.75	6.61	5.54	7.82	6.59	4.72	3.98
Industrial area	1.31	1.10	0.31	0.26	1.65	1.39	3.01	2.54
Water bodies	3.89	3.26	2.79	2.34	4.27	3.60	1.53	1.29
Barren land	2.68	2.24	5.69	4.77	3.83	3.23	0.59	0.50

Table 5. Lan duse and land cover change of Churulia mining region (1991-2021)

LULC classes	1991		2001		2011		2021	
	Area (km^2)	Area (%)	Area (km^2)	Area (%)	Area (km^2)	Area (%)	Area (km^2)	Area (%)
Vegetation	14.68	13.19	10.29	9.20	9.63	8.59	9.08	8.12
Built-up area	3.59	3.23	4.13	3.69	7.39	6.59	17.73	15.86
Agricultural land	75.69	68.01	73.15	65.41	70.72	63.08	68.95	61.68
Mining area	1.98	1.78	2.96	2.65	9.52	8.49	10.60	9.48
Industrial area	0.10	0.09	0.40	0.36	0.87	0.78	1.11	0.99
Water bodies	1.56	1.40	1.46	1.31	1.47	1.31	1.21	1.08
Barren land	13.69	12.30	19.45	17.39	12.52	11.17	4.19	3.75

primarily caused by mining and built-up activities. The vegetation cover of this region occupied 15.31% in 1991, 9.26% in 2001, 5.95% in 2011, and 3.58% of the area in 2021, showing a rapid decreasing trend. Growth of built-up area was fast in the south and central part of this region, which became the most populated area of the Paschim Bardhaman district. The built-up area increased by 19.85% between 1991 and 2021. Agricultural land decreased and converted into settlement, mining, and industrial regions. In 1991, 49.94% of the land was under agricultural land use. It increased to 53.50% in 2001. However, after 2001, agricultural land gradually decreased to 44.15% in 2011 and 37.02% in 2021. Mining activity expanded rapidly. Only 3.94% of the land was occupied by coal mines in 1991, which were also very scattered. However, after starting a new opencast coal mine in the Sonepur-Bazari region, it expanded dramatically into agricultural land and natural vegetation. 5.64, 5.94 and 8.03% of the region was covered by coal mines, respectively, in 2001, 2011 and 2021. The industrial region also increased rapidly, from 0.8% in 1991 to 1.50% in 2001. However, in 2011, it increased to 5.62%, and in 2021, 6.79% of land was converted to an industrial area due to the opening of a new steel and power plant industrial hub at Jamuria. Water bodies decreased from 3.38% in 1991 to 1.54% in 2001, 0.52% in 2011, and 0.81% in 2021. Barren land was maximum in 2011 (11.58%) but drastically decreased to 5.05% in 2021. Maximum portion of the Barren land was converted to coal mines and settlement (Table 6, Fig. 8).

Durgapur UHI and LULC (1991-2021)

From 1991 to 2021, the Durgapur urban-industrial zone experienced a gradual increase in surface temperature from 31.25 to 37°C. This region is Paschim Bardhaman district's second most densely inhabited area and is a planned city. The cross-section I-J area runs through the industrial and settlement zones in the core area and buffer region. The temperature gradient is much more significant in the industrial region than in the surrounding agricultural and vegetation areas (Fig. 9).

The vegetation cover of the region decreased mainly in the southern part, 22.93% in 1991, 14.69% in 2001, 14.00% in 2011, and 8.39% in 2021. Built-

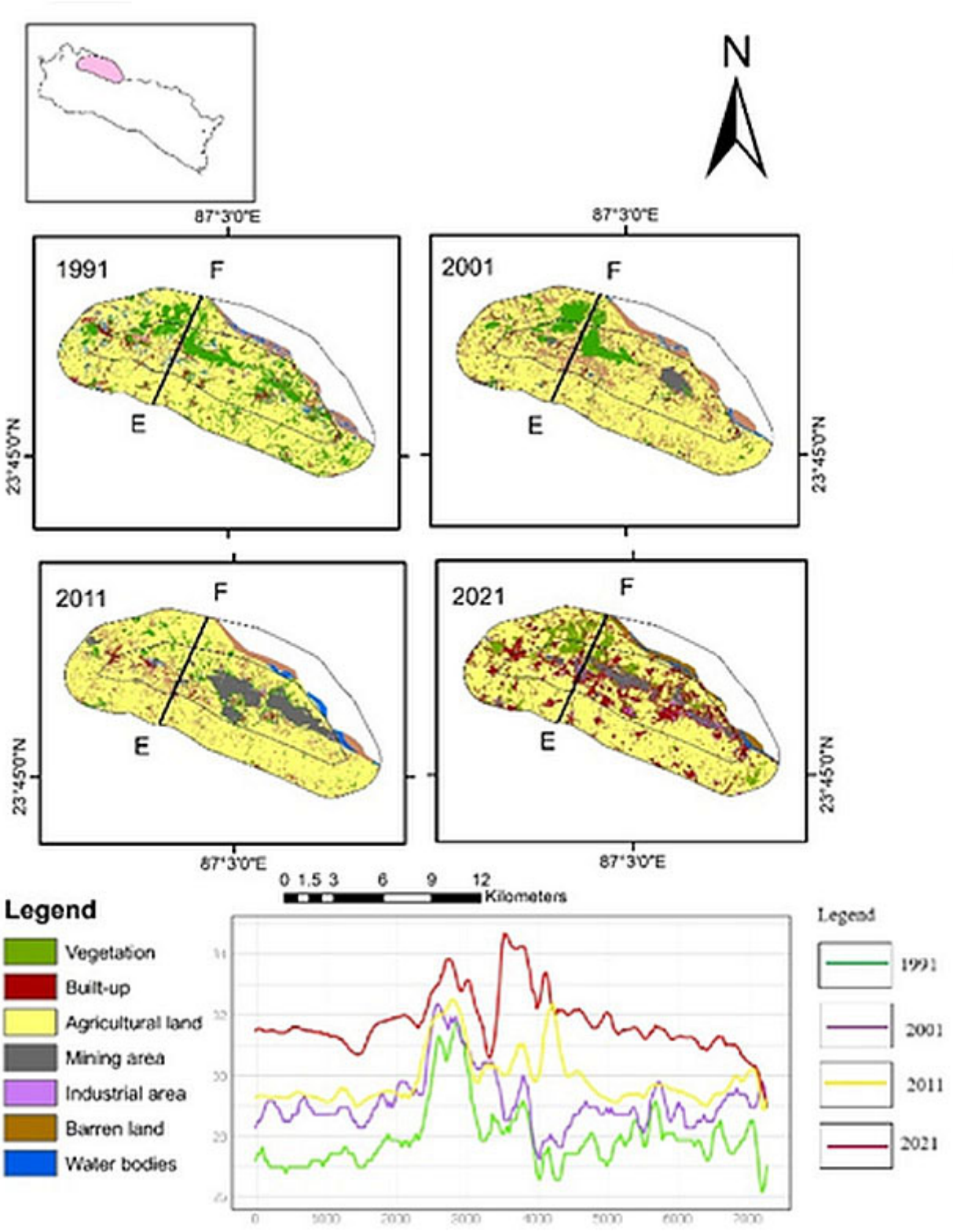

Figure 7. UHI map of Churulia region (1991 to 2021)

up area increased rapidly, expanding from the core to the peripheral zone of Durgapur city from 28.20% in 1991 to 33.20% in 2001, 40.91% in 2011, and 48.58% in 2021. Agricultural land increased from 35.16% in 1991 to 36.74% in 2001, at the expense of dense vegetation. It decreased to 25.86% in 2011 and 21.19% in 2021, mainly in the northern and eastern parts. Since 1907, this region has been famous for being home to the country's heavy iron and steel industries — Tata Steel, Durgapur Steel plant, Alloy

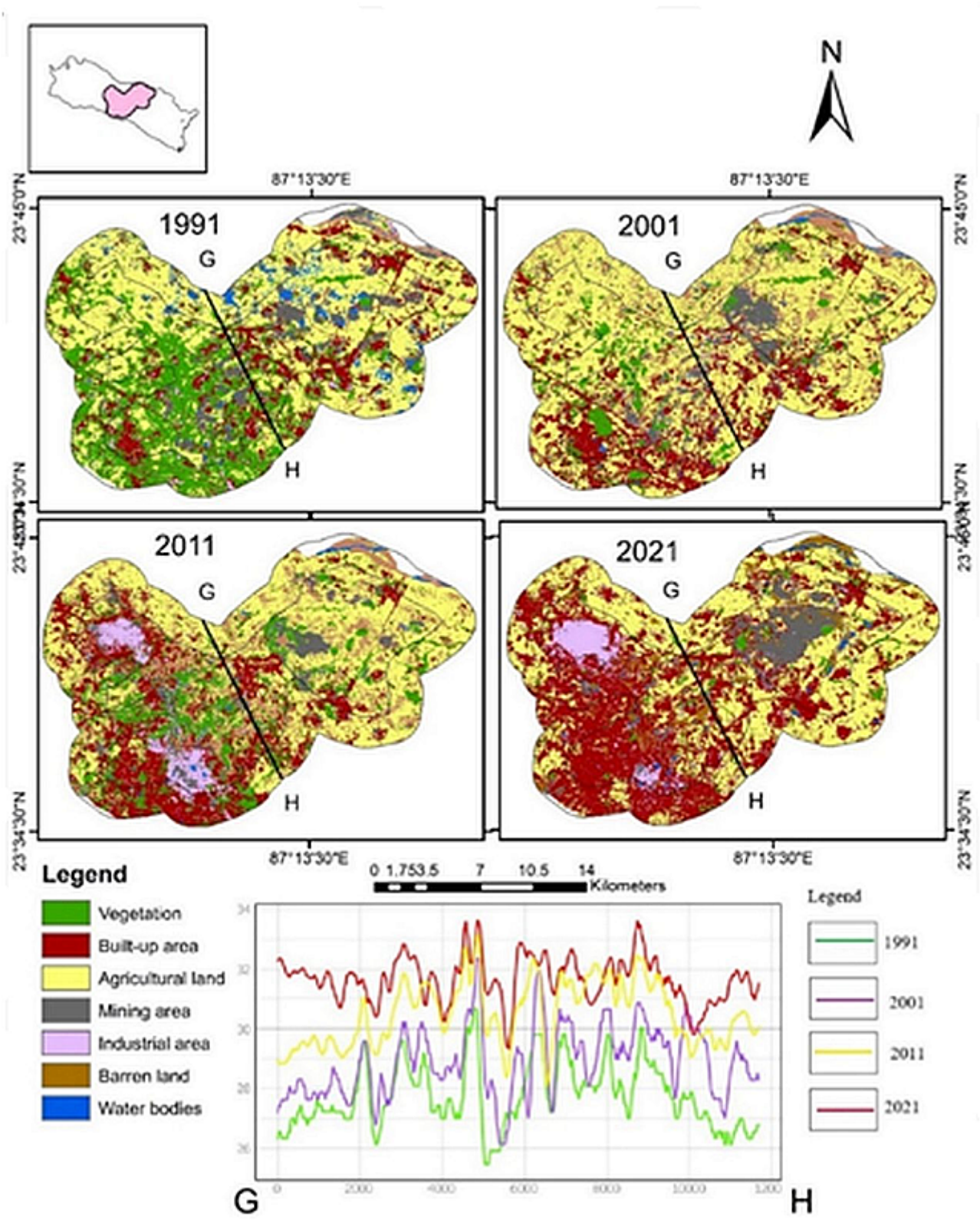

Figure 8. UHI map of Raniganj-Andal region 1991 to 2021

Steel Plant, Durgapur Chemicals, Bharat Electronics, etc. Industrial area increased on the bank of Damodar River from 4.55% in 1991 to 8.76% in 2001, 14.10% in 2011, and 16.40% in 2021. Water bodies and barren land decreased gradually from 1991 to 2021 (Table 7, Fig. 9).

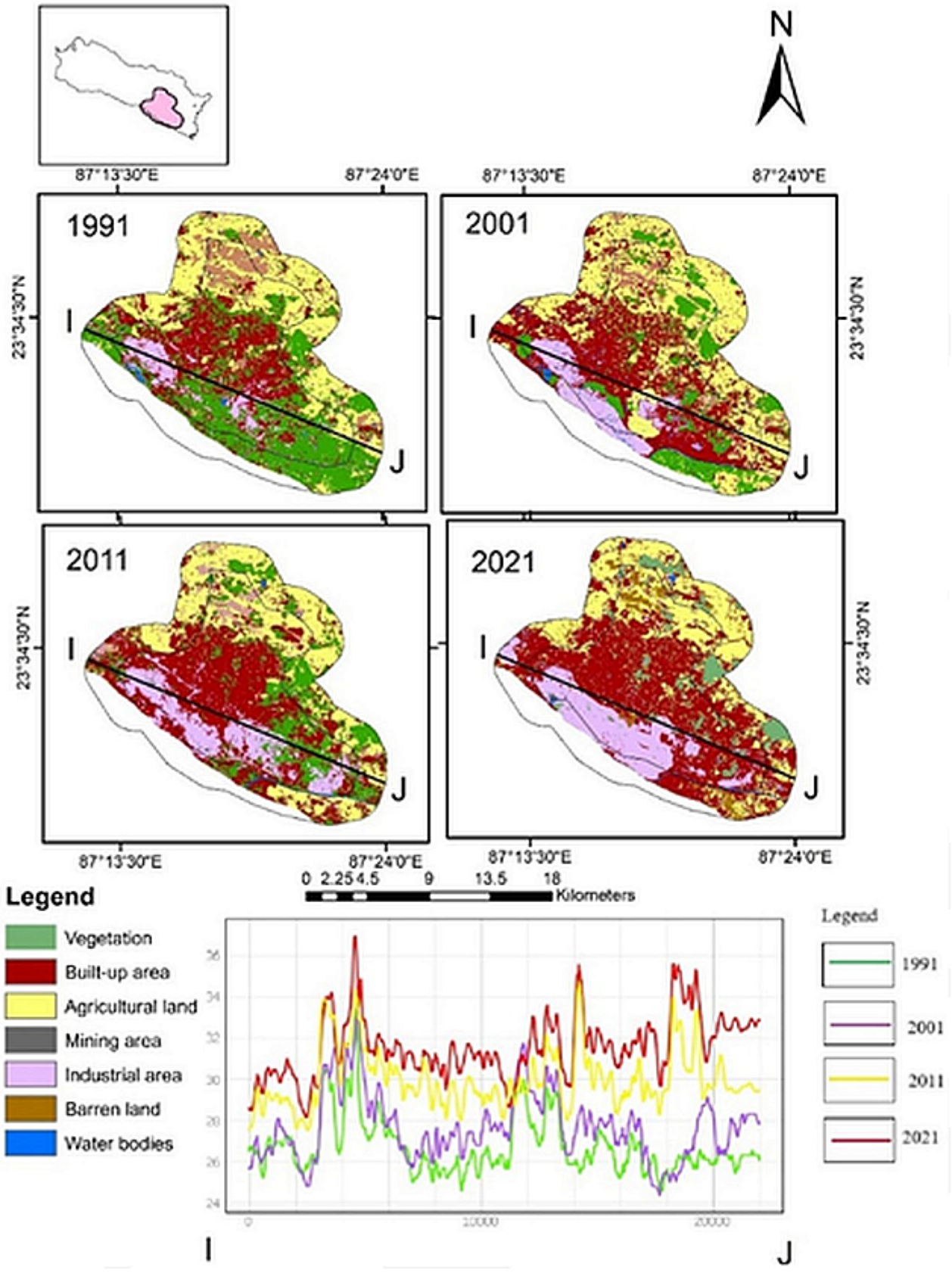

Figure 9. UHI map of Durgapur region (1991 to 2021)

Table 6. Land use and land cover change of Andal-Raniganj region (1991- 2021)

LULC classes	1991		2001		2011		2021	
	Area (km^2)	Area (%)	Area (km^2)	Area (%)	Area (km^2)	Area (%)	Area (km^2)	Area (%)
Vegetation	49.25	15.31	29.71	9.26	19.11	5.95	12.36	3.85
Built-up area	59.86	18.60	63.88	19.90	84.25	26.24	123.56	38.45
Agricultural land	160.69	49.94	171.72	53.50	141.74	44.15	118.97	37.02
Mining area	12.69	3.94	18.12	5.64	19.07	5.94	25.81	8.03
Industrial area	2.56	0.80	4.83	1.50	18.04	5.62	21.81	6.79
Water bodies	10.87	3.38	4.94	1.54	1.66	0.52	2.61	0.81
Barren land	25.87	8.04	27.83	8.67	37.17	11.58	16.23	5.05

Table 7. Land use and land cover change of Durgapur area (1991- 2021)

LULC classes	1991		2001		2011		2021	
	Area (km^2)	Area (%)	Area (km^2)	Area (%)	Area (km^2)	Area (%)	Area (km^2)	Area (%)
Vegetation	52.68	22.93	33.79	14.69	32.34	14.00	19.30	8.39
Built-up area	64.78	28.20	76.36	33.20	94.52	40.91	111.69	48.58
Agricultural land	80.79	35.16	84.49	36.74	59.74	25.86	48.71	21.19
Mining area	1.04	0.45	1.08	0.47	1.02	0.44	1.89	0.82
Industrial area	10.45	4.55	20.14	8.76	32.57	14.10	37.70	16.40
Water bodies	4.65	2.02	4.94	2.15	1.03	0.45	1.22	0.53
Barren land	15.36	6.69	9.18	3.99	8.81	3.81	9.39	4.08

Spatio-temporal variation of ecological evaluation in Paschim Bardhaman district through UTFVI for the years 1991, 2001, 2011 and 2021

The spatiotemporal variations of ecological deterioration in Paschim Bardhaman district are shown for 1991, 2001, 2011, and 2021 with the help of surface temperature data through the UTFVI technique. Ecological deterioration is classified into six categories based on the ecological index and its values. They are excellent (<0), good (0 to 0.005), normal (0.005 to 0.010), bad (0.010 to 0.015), worse (0.015 to 0.020) and worst (>0.020) (Yong et al., 2006; Rashid et al., 2022). In 1991, the ecological index was 'excellent' (10.44%) in the forest area of Kanksa block, followed by 'good' and 'normal' ecological index at 60.07%. However, most of the area fell under this category, and 29% occupied the 'bad,' 'worse,' and 'worst' categories since these areas are located near industrial and mining areas. In 2001, the majority of the area fell under the normal ecological index, which is 34.23%. The 'excellent' and 'good' ecological conditions were observed in 30.7% area, while the areas in the 'bad,' 'worse', and 'worst' categories increased by 35.07%. There is a noticeable increase in the area, with worse ecological conditions near the industrial area of Asansol city and the newly opened coal mines region. In 2011, 6.70% and 29.59% of areas fell under the 'excellent' and 'good' categories, which decreased significantly from previous decades, and 38.29% are under 'bad,' 'worse', and 'worst' ecological conditions. The reduction in areas with excellent and good ecological categories is due to increased built-up areas in cities' outskirts and the continuous opening of coal mines. In 2021, the excellent (5.95%) and good (26.18%) ecological areas decreased dramatically, while the bad, worse, and worst areas grew by 40.57%. The trend of the ecological assessment index reflects the current level of environmental degradation and UHI severity. The temperature in the central region of the city has been rising due to the large concentration of built-up area. It can be clearly defined that due to the high concentration of the built-up area, the temperature has been increasing in the central part of the region. Overall ecological index showing from 1991 to 2021, the 'excellent' ecological areas decreased from 10.44% to 5.95% (4.49%) but 'bad' 'worse' and

Table 8. Decadal change of ecological evaluation index for the years 1991 to 2021

UTFVI threshold value	UHI phenomena	Ecological Evaluation Index	1991		2001		2011		2021	
			Area (km^2)	Area (%)	Area (km^2)	Area (%)	Area (km^2)	Area (%)	Area (km^2)	Area (%)
<0	None	Excellent	168.3	10.44	116.74	7.24	107.97	6.70	95.96	5.95
0.000-0.005	Weak	Good	435.95	27.05	378.11	23.46	475.88	29.53	421.86	26.18
0.005-0.010	Middle	Normal	532.1	33.02	551.53	34.23	410.22	25.46	439.67	27.28
0.010-0.015	Strong	Bad	310.21	19.25	320.43	19.89	328.80	20.40	343.93	21.34
0.015-0.020	Stronger	Worse	136.13	8.45	212.99	13.22	248.35	15.41	266.43	16.53
>0.020	Strongest	Worst	28.71	1.78	31.61	1.96	39.95	2.48	43.56	2.70

'worst' areas increased abnormally from 29.75% to 40.59% (10.84%) and remaining 'good' and 'normal' areas also decreased from 60.07 to 53.46% (6.61%) (Table 8, Fig. 10).

Heat Risk Index Assessment of Paschim Bardhaman District for the year 2021

The increase in the number and severity of weather extremes, including excessive heat waves potentially associated with climate change has highlighted the need for research into risk assessment and risk reduction measures. Extreme heat events have been consistently reported as the leading cause of weather-related mortality in India in recent years. Paschim Bardhaman district experienced 153 heat waves days from 1969-2019, and from 2019-2023, 44 days experienced heat waves (Indian Meteorological Department of India). In order to fully understand impact potentials and analyze risk in its components, both the spatially and temporally varying patterns of heat and the multidimensional characteristics of vulnerability have to be considered. Risk patterns are driven by the geographic variations of vulnerability, generally showing a clear difference between high-risk urban areas and low-risk in suburban and rural environments. Since risk is considered an aggregate measure of hazard and vulnerability, we set heat stress risk for this study as a function of the modelled heat stress and heat-related vulnerability described above. The impacts of extreme heat events must be attributed to changes in these aspects. The multiplication of these two equally weighted risk components defines the Heat Risk Index (HRI) score. Modelling current patterns of heat-related risk can improve our understanding of underlying causes of heat stress and inherent vulnerability interaction in creating adverse effects for human beings (Aubrecht and Özceylan 2013, Yardley et al. 2011). A weighted overlay analysis was done on the GIS platform to evaluate the Heat Risk Index (HRI). A 1 km grided population density of the study area was used for vegetation cover NDVI and temperature analysis. The average land surface temperature was used. Only 2.69% (42.35 km2) of the area fell under the very low-risk zone category, and 30.69%, which covered 481.99 km2, fell under the low-risk zone. Maximum (782.46 km2) part of the study area (more or less 50%) experienced moderate heat risk. Maximum agricultural land, which has a moderately low population density compared to the city area, experiences moderate heat risk. Outer parts of Asansol city, Raniganj, Andal, and Durgapur are more vulnerable, occupying 14.92% of the district (Table 9, Fig. 11). Core part of Asansol city and Kulti, where population density is high, due to over-dense built-up area poor air circulation, heavy traffic this area experienced very high heat risk.

In 1991, 2.11% of the study area experienced less than 25°C, with 41.33% area falling between 25-27°C. The southeastern part of the study area experienced the highest temperatures (47.22% area),

Table 9. Heat risk categories for the year 2021

Categories	**Area (km^2)**	**Area (%)**
Very low risk	42.3531	2.692515
Low risk	481.9959	30.64194
Moderate risk	782.4609	49.74341
High risk	234.7875	14.92615
Very high risk	31.3965	1.995971

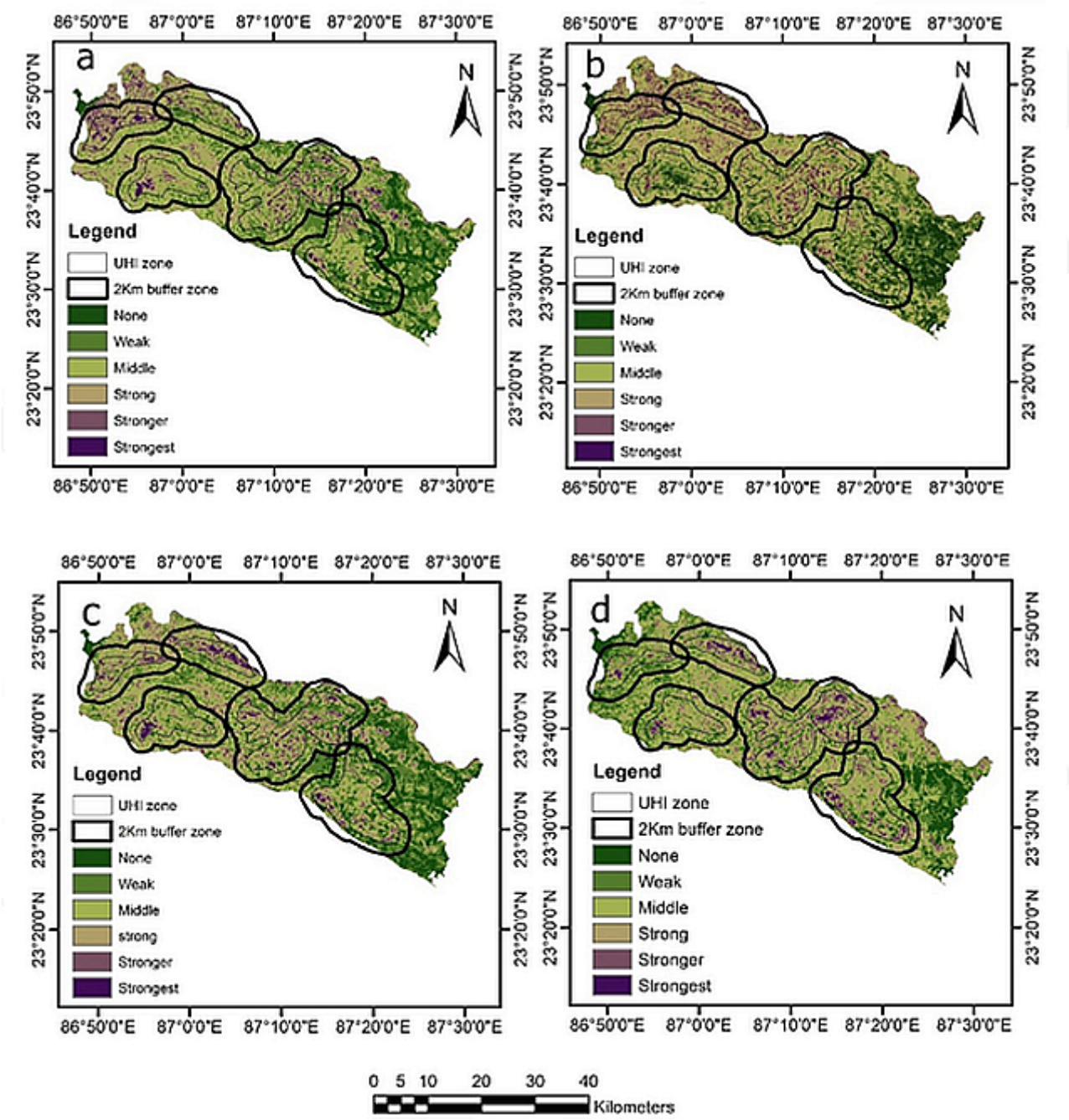

Figure 10. Urban Thermal Field Variance Index (a.1991, b. 2001, c. 2011, d.2021)

with only 8.69% area reaching 31°C. In 2001, areas under 25 and 27°C declined by 0.56 and 22.07%, respectively. In 2011, over 60% of the area experienced more than 29°C LST. High temperatures increased rapidly in the core city region and mining area. In 2021, 0.58% of the area experienced less than 27°C, while area under 29-31°C decreased from 60.70 to 36.53%. In 2021, 4.36% of area experienced higher than 33°C, and 0.46% area experienced more than 35°C LST. The highest LST levels were reported at night in Asansol and Durgapur city. The vegetation cover in the area decreased by 21.13%, while the built-up and industrial areas increased by 29.5 and 2.54%, respectively. The LST in the Asansol region has increased by 36°C, as also in the neighbouring industrial region. Between 1991 and 2021, the built-up area in the Salanpur-Kulti region expanded by 23.92%, while the mining area increased by 1.84% as the number of operational coal mines declined. More than 34°C LST was recorded in the adjacent

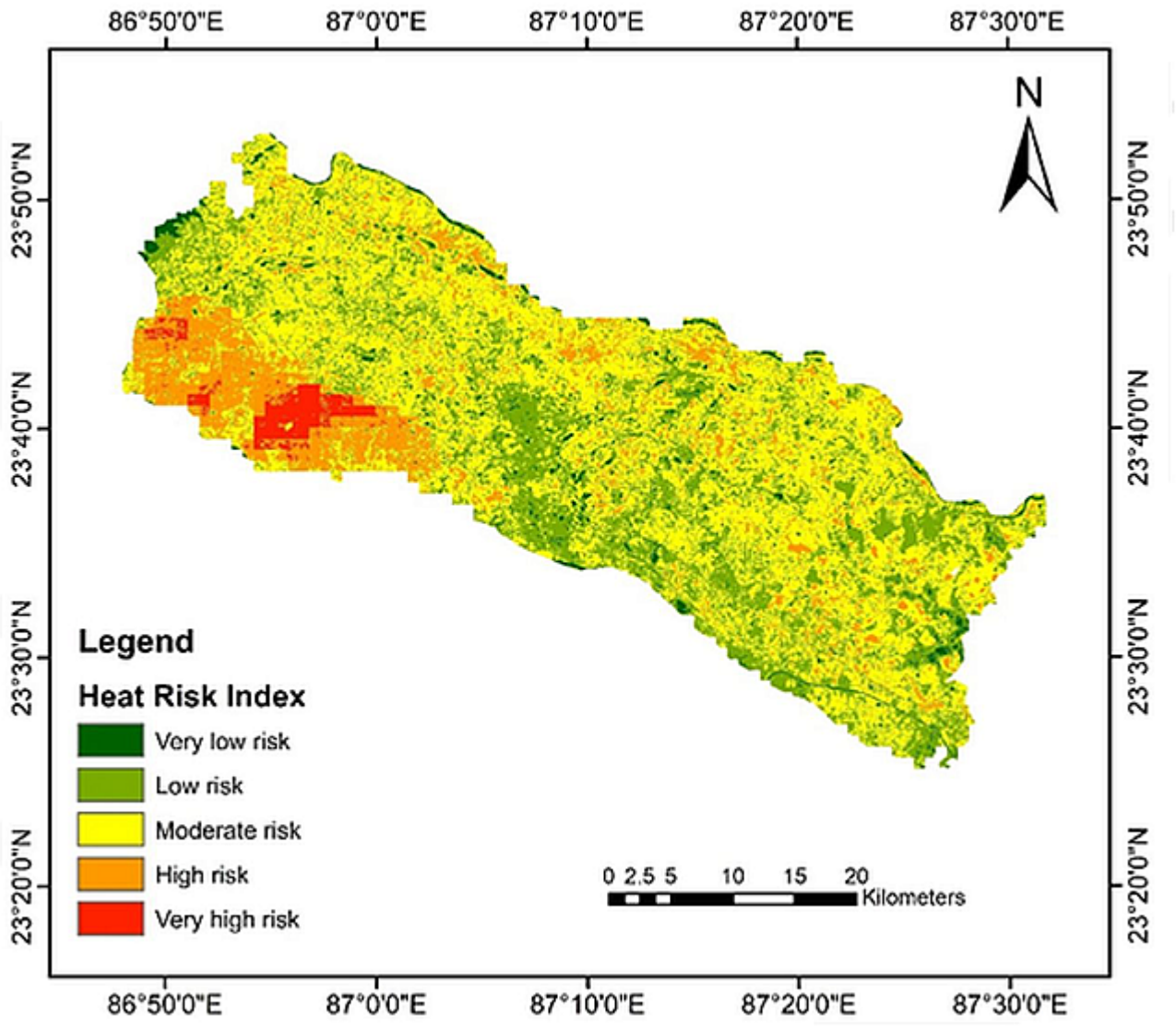

Figure 11. Heat Risk Index of 2021

mining area. In Churulia, plant cover declined by 5.07% over the last 30 years. From 1991 to 2021, the mining area rose by 7.7%. Due to this, the LST in this area increased by 35°C. In the south-western part of the Raniganj-Andal area, a maximum portion of land was converted into settlement (19.85%) and industrial (5.98%) regions. Mining area increased in the last three decades by 4.9%. Historically, the Durgapur area was known as an urban industrial region. Industrial area increased by 11.85% and built-up area by 20.38% from 1991 to 2021. Maximum LST increased to 37°C from 1991 to 2021. In 1991, the UHI zone covered 14% of the total study area, which increased by 23% in 2021. In only 30 years, 9% of the UHI area increased. Asansol urban-industrial region, Salanpur-Kulti region, Churulia mining region, Andal-Raniganj region, and Durgapur region experience UHI phenomena with changing land use land and cover patterns. High UTFVI makes the city more uncomfortable and non-environmental friendly; high UTFVI areas were increased, particularly in Asansol, Durgapur, and the Andal region, due to increased industrial and mining activity. The Ecological index shows from 1991 to 2021, the 'excellent' ecological areas decreased by 4.49%, but 'bad' 'worse' and 'worst' areas increased abnormally by 10.84%, and 'good' and 'normal' areas also decreased by 6.61%. Only 2.69% (42.35 km^2) of the region fell into the very low-risk area category, while 30.69% (481.99 km^2) fell into the

low-risk zone. Most of the research region, around 50%, or 782.46 km^2, is subject to moderate heat risk. Most agricultural terrain with a lower population density than the city region is exposed to mild heat. The outside parts of Asansol city, Raniganj, Andal, and Durgapur are more vulnerable, occupying 14.92% of the district. Core parts of Asansol city and Kulti face very high heat risk where population density is high due to overcrowded built-up areas, inadequate air circulation, and excessive traffic.

CONCLUSIONS

Urban surfaces such as concrete and asphalt, which collect more heat than their rural counterparts, have higher thermal inertia. In this study area, prominent industrial regions and opencast mines contribute to additional environmental concerns. Asansol and Durgapur form a rising urban agglomeration in eastern India. The rapid conversion of agricultural land to developed areas, mining, and industry significantly impacts the city's ecosystem. Urban heat island phenomena have increased twice since 1991, whereas the degree of urban thermal comfort has decreased over the previous 30 decades. The CBD section of the district had the highest heat risk compared to the other planned areas due to its unplanned and densely inhabited nature.

ACKNOWLEDGEMENTS

The authors acknowledge USGS for free satellite images for the research work and the first author expressed thanks to UGC, New Delhi for providing JRF fellowship.

Authors' contributions: All authors contributed equally.

Conflict of interest: Authors declare that they have no conflict of interest.

REFERENCES

Amiri, R., Weng, Q., Alimohammadi, A. and Alavipanah, S.K. 2009. Spatial-temporal dynamics of land surface temperature in relation to fractional vegetation cover and land use/cover in the Tabriz urban area, Iran. Remote Sensing of Environment, 113(12), 2606-2617. https://doi.org/10.1016/j.rse.2009.07.021

Anonymous. 2015. Asansol Durgapur Development Authority. http://addaonline.in/adda-at-a-glance

Aubrecht, C. and Özceylan, D. 2013. Identification of heat risk patterns in the US National Capital Region by integrating heat stress and related vulnerability. Environment International, 56, 69-77. https://doi.org/10.1016/j.envint.2013.03.005

Barata, M., Ligeti, E., De Simone, G., Dickinson, T., Jack, D., Penney, J., Rahaman, M., and Zimmerman, R. 2011. Climate change and human health in cities. Pp. 179-213. In: Rosenzweig, C., Solecki, W.D., Hammer, S.A. and Mehrotra, S. (Eds.). Climate Change and Cities First Assessment Report of the Urban Climate Change Research Network, Cambridge University Press, Cambridge.

Bhatta, B. 2009. Analysis of urban growth pattern using remote sensing and GIS: a case study of Kolkata India. International Journal of Remote Sensing, 30(18), 4733-4746. https://doi.org/10.1080/01431160802651967

Cevik Degerli, B. and Cetin, M. 2023. Evaluation of UTFVI index effect on climate change in terms of urbanization. Environmental Science and Pollution Research, 30(30), 75273-75280. https://doi.org/10.1007/s11356-023-27613-x

Chakma, A., Krishnaiah, Y.V., Panja, K., Mallick, M., Rai, D., Das, D. and Hati, M. 2023. Evaluation of seasonal variation in water quality in Agartala City, India using principal component analysis and water quality index. International Journal of Ecology and Environmental Sciences, 49, 485-495. https://doi.org/10.55863/ijees.2023.2839

Chatterjee, S. and Gupta, K. 2021. Exploring the spatial pattern of urban heat island formation in relation to land transformation: A study on a mining industrial region of West Bengal, India. Remote Sensing Applications: Society and Environment, 23, 100581. https://doi.org/10.1016/j.rsase.2021.100581

Das, N., Mondal, P., Sutradhar, S. and Ghosh, R. 2021. Assessment of variation of land use/land cover and its impact on land surface temperature of Asansol subdivision. The Egyptian Journal of Remote Sensing and Space Science, 24(1), 131-149. https://doi.org/10.1016/j.ejrs.2020.05.001

Fahmy, A. H., Abdelfatah, M. A., & El-Fiky, G. 2023. Investigating land use land cover changes and their effects on land surface temperature and urban heat islands in Sharqiyah Governorate, Egypt. The Egyptian Journal of Remote Sensing and Space Science, 26(2), 293-306. https://doi.org/10.1016/j.ejrs.2023.04.001

Fouillet, A., Rey, G., Wagner, V., Laaidi, K., Empereur-Bissonnet, P., Le Tertre, A., Terte, A., Frayssinet, P., Bessemoulin, P., Laurent, F., Crouy-Chanel, De, E., Jougla, E. and Hémon, D. 2008. Has the impact of heat waves on mortality changed in France since the European heat wave of summer of 2003 A study of the 2006 heat wave. International Journal of Epidemiology, 37(2), 309-317. https://doi.org/10.1093/ije/dym253

Gazi, M.A.A. and Mondal, I. 2018. Urban heat island and its

effect on dweller of Kolkata metropolitan area using geospatial techniques. International Journal of Computer Sciences and Engineering, 6(10), 741-753. https://doi.org/10.26438/ijcse/v6i10.741753

Guha, S., Govil, H., Dey, A., Gill, N. 2018. Analytical Study of Land Surface Temperature with NDVI and NDBI Using Landsat 8 OLI and TIRS Data in Florence and Naples City, Italy. European Journal Remote Sensing 51 (1), 667–678. https://doi.org/10.1080/22797254.2018.1474494

Gupta, K., Dey, A. and Mondal, B. 2019. Geoinformatics based techniques for the study of spatialization of urban heat island and micro-climatic region in Asansol Durgapur Development Authority, West Bengal. Pp. 361. In: Basu, M., Gupta, A.D., Mondal, B.K. and Bhattacharyya, D. (Eds.). Geo-Environmental Issues of the New Millennium-Sustainable Planning Perspective. Dey's Publishing, Kolkata.

Gupta, R.K. 2024. Green space cooling to ditigate the surface urban heat island effect in India's metropolises. Current World Environment, 19(2), 679-691. http://dx.doi.org/10.12944/CWE.19.2.13

Halder, B., Bandyopadhyay, J., Khedher, K.M., Fai, C.M., Tangang, F. and Yaseen, Z.M. 2022. Delineation of urban expansion influences urban heat islands and natural environment using remote sensing and GIS-based in industrial area. Environmental Science and Pollution Research, 29(48), 73147-73170. https://doi.org/10.1007/s11356-022-20821-x

Hota, P. and Behera, B. 2015. Coal mining in Odisha: an analysis of impacts on agricultural production and human health. The Extractive Industries and Society, 2(4), 683-693. https://doi.org/10.1016/j.exis.2015.08.007

Imran, H.M., Hossain, A., Islam, A.S., Rahman, A., Bhuiyan, M.A.E., Paul, S. and Alam, A. 2021. Impact of land cover changes on land surface temperature and human thermal comfort in Dhaka city of Bangladesh. Earth Systems and Environment, 5, 667-693. https://doi.org/10.1007/s41748-021-00243-4

Jauregui, E., Godinez, L. and Cruz, F. 1992. Aspects of heat-island development in Guadalajara, Mexico. Atmospheric Environment – Part B Urban Atmosphere, 26B, 391-396. https://doi.org/10.1016/0957-1272(92)90014-j

Karaca, M., Tayanc, M. and Toros, H. 1995. Effects of urbanization on climate of Istanbul and Ankara. Atmospheric Environment, 29(23), 3411-3421. https://doi.org/10.1016/1352-2310(95)00085-D

Kikon, N., Singh, P., Singh, S.K. and Vyas, A. 2016. Assessment of urban heat islands (UHI) of Noida City, India using multi-temporal satellite data. Sustainable Cities and Society, 22, 19-28. https://doi.org/10.1016/j.scs.2016.01.005

Koshal, A.K. 2002. Environmental Problems Analysis of Coal Mining in Raniganj and Asansol Blocks (West Bengal) Using Remote Sensing and GIS. GIS Development. http://admin.indiaenvironmentportal.org.in/files/COAL%20MINING.pdf

Krishnaiah, Y.V. 2013. Landuse pattern and land use efficiency of the Papagni river basin, India. The Indian Journal of Spatial Science, 4(1), 59-68.

Kumar, R., Mishra, V., Buzan, J., Kumar, R., Shindell, D. and Huber, M. 2017. Dominant control of agriculture and irrigation on urban heat island in India. Scientific Reports, 7(1), 1-10. https://doi.org/10.1038/s41598-017-14213-2

Maity, B., Mallick, S.K. and Rudra, S. 2020. Spatiotemporal dynamics of urban landscape in Asansol municipal corporation, West Bengal, India: a geospatial analysis. Geojournal, 87, 1619-1637. https://doi.org/10.1007/s10708-020-10315-z

Mallick, M. and Krishnaiah Y.V. 2023. Spatio-temporal detection of land use land cover changes in Jalpaiguri district; Geospatial analysis. International Journal of Science Research, 12(12), 1945-1953. https://doi.org/10.21275/sr231227231047

Mallick, M., Krishnaiah, Y.V., Panja, K., Das, D., Rai, D., Hati, M. and Chakma, A. 2024. Land suitability assessment for tea cultivation in Jalpaiguri district of West Bengal, India, using AHP and DEMATEL techniques. Environment, Development and Sustainability, 2024, 1-39. https://doi.org/10.1007/s10668-024-05711-1

Mallick, M., Krishnaiah, Y.V., Panja, K., Das, D., Rai, D., Hati, M. and Chakma, A. 2025. Assessment of the soil erosion susceptibility zones in tea plantation areas of Jalpaiguri District, India: An integrated approach of RUSLE and WLC model. Journal of Indian Society of Remote Sensing, (in press). https://doi.org/10.1007/s12524-024-02078-8

Mathew, A., Khandelwal, S. and Kaul, N. 2016. Spatial and temporal variations of urban heat island effect and the effect of percentage impervious surface area and elevation on land surface temperature: Study of Chandigarh city, India. Sustainable Cities and Society, 26, 264-27. https://doi.org/10.1016/j.scs.2016.06.018

Mohan, M., Singh, V.K., Bhati, S., Lodhi, N., Sati, A.P., Sahoo, N.R. and Dey, S. 2020. Industrial heat island: A case study of Angul-Talcher region in India. Theoretical and Applied Climatology, 141(1), 229-246. https://doi.org/10.1007/s00704-020-03181-9

Oke, T.R. 1973. City size and the urban heat island. Atmospheric Environment, 7(8), 769-779. https://doi.org/10.1016/0004-6981(73)90140-6

Oke, T.R. 1995. The heat island of the urban boundary layer: characteristics, causes and effects. Pp. 81-107. In: Cermak, J.E., Davenport, A.G., Plate, E.J. and Viegas, D.X. (Eds.). Wind Climate in Cities. NATO ASI Series, volume 277. Springer, Dordrecht. https://doi.org/10.1007/978-94-017-3686-2_5

Panja, K., Krishnaiah, Y.V., Chakma, A., Mallick, M., Rai, D., Hati, M. and Das, D. 2023. Impact of rubber plantation growth on LULC changes in eastern-Himalayan region of West Tripura District using geospatial approach. International Journal of Ecology and Environmental Sciences, 49(5), 533-548. https://doi.org/10.55863/ijees.2023.2852

Paterson, J.C.K 1910. Bengal District Gazetteers: Burdwan, Bengal Secretariat Book Depot, Calcutta.

Patra, T., Dutta, D., Kundu, A., Kumar, M., Hossain, S.S. and

Chattoraj, K.K. 2022. Evolution of opencast mines in the Raniganj Coalfield (India): An assessment through multi-temporal satellite data. Journal of the Geological Society of India, 98(3), 387-394. https://doi.org/10.1007/s12594-022-1990-5

Pu, R., Gong, P., Michishita, R. and Sasagawa, T. 2006. Assessment of multi-resolution and multi-sensor data for urban surface temperature retrieval. Remote Sensing of Environment, 104(2), 211-225. https://doi.org/10.1016/j.rse.2005.09.022

Rashid, N., Alam, J.M., Chowdhury, M.A. and Islam, S.L.U. 2022. Impact of land use change and urbanization on urban heat island effect in Narayanganj city, Bangladesh: A remote sensing-based estimation. Environmental Challenges, 8, 100571. https://doi.org/10.1016/j.envc.2022.100571

Shahfahad, Talukdar, S., Rihan, M., Hang, H.T., Bhaskaran, S. and Rahman, A. 2022. Modelling urban heat island (UHI) and thermal field variation and their relationship with land use indices over Delhi and Mumbai metro cities. Environment, Development and Sustainability, 24(3), 3762-3790. https://doi.org/10.1007/s10668-021-01587-7

Shastri, H. and Ghosh, S. 2019. Urbanisation and surface urban heat island intensity (SUHII). Pp. 73-90. In: Venkataraman, C., Mishra, T., Ghosh, S. and Karmakar, S. (Eds.). Climate Change Signals and Response. Springer, Singapore. https://doi.org/10.1007/978-981-13-0280-0_5

Siddique, G., Roy, A., Mandal, M.H., Ghosh, S., Basak, A., Singh, M. and Mukherjee, N. 2022. An assessment on the changing status of urban green space in Asansol city, West Bengal. GeoJournal, 87(2), 1299-1321. https://doi.org/10.1007/s10708-020-10312-2

Siebert, S., Webber, H., Zhao, G. and Ewert, F. 2017. Heat stress is overestimated in climate impact studies for irrigated agriculture. Environmental Research Letters, 12(5), 054023. https://doi.org/10.1088/1748-9326/aa702f

Sultana, S. and Satyanarayana, A.N.V. 2019. Impact of urbanization on urban heat island intensity during summer and winter over Indian metropolitan cities. Environmental Monitoring and Assessment, 191(3), art 789. https://doi.org/10.1007/s10661-019-7692-9

Tan, J., Zheng, Y., Tang, X., Guo, C., Li, L., Song, G. and Chen, H. 2010. The urban heat island and its impact on heat waves and human health in Shanghai. International Journal of Biometeorology, 54(1), 75-84. https://doi.org/10.1007/s00484-009-0256-x

Wang, N., Xia, J., Yin, J. and Liu, X. 2016. Trend analysis of land surface temperatures using time series segmentation algorithm. Journal of Intelligent and Fuzzy Systems, 31(2), 1121-1131. https://doi.org/10.3233/JIFS-169041

Yague, C., Zurita, E. and Martinez, A. 1991. Statistical analysis of the Madrid urban heat island. Atmospheric Environment – Part B Urban Atmosphere, 25, 327-332. https://doi.org/10.1016/0957-1272(91)90004-X

Yang, B., Meng, F., Ke, X. and Ma, C. 2015. The impact analysis of water body landscape pattern on urban heat island: a case study of Wuhan City. Advances in Meteorology, 2015, Article ID 416728. https://doi.org/10.1155/2015/416728

Yardley, J., Sigal, R.J. and Kenny, G.P. 2011. Heat health planning: The importance of social and community factors. Global Environmental Change, 21(2), 670-679. https://doi.org/10.1016/j.gloenvcha.2010.11.010

Yong, Z., Tao, Y., Gu, X-F., Zhang, Y-X., Yu, S., Zhang, W-J. and Li, X. 2006. Land surface temperature retrieval from cbers-02 irmss thermal infrared data and its applications in quantitative analysis of urban heat island effect. National Remote Sensing Bulletin, 10(5), 789-797. https://doi.org/10.11834/jrs.200605117 (in chinese)

Zhou, D., Zhao, S., Zhang, L., Sun, G. and Liu, Y. 2015. The footprint of urban heat island effect in China. Scientific Reports, 5(1), 11160. https://doi.org/10.1038/srep11160

Zhou, Y., Zhao, H., Mao, S., Zhang, G., Jin, Y., Luo, Y. and Lun, F. 2022. Exploring surface urban heat island (SUHI) intensity and its implications based on urban 3D neighbourhood metrics: An investigation of 57 Chinese cities. Science of the Total Environment, 847, 157662. https://doi.org/10.1016/j.scitotenv.2022.157662

Received:30th January 2025
Accepted: 24th May 2025